Acquisition of a Complex OBN survey in the Balder-Ringhorne area of the North Sea

Introduction

The Norwegian North Sea is a prolific hydrocarbon province with large oil and gas fields such as Ekofisk, Troll, Statfjord, Oseberg, and Johan Sverdrup. Whereas ocean bottom node (OBN) seismic has been shown to have benefits over streamer seismic e.g. in terms of number of recorded components, offsets, azimuths, and samples per area (Jansen et al., 2021), the use of OBN in the offshore oil and gas industry has historically been restricted to small proprietary surveys over producing oil and gas fields for 4D monitoring purposes. Since 2018, several large OBN surveys have been acquired in mature areas of the North Sea driven by a need for improved data quality in infrastructure-led exploration (ILX).

The Heimdal Terrace OBN survey was acquired over the producing Balder and Ringhorne fields and near-field exploration acreage to the west in the North Sea in the period from March to June 2023 (Figure 1).

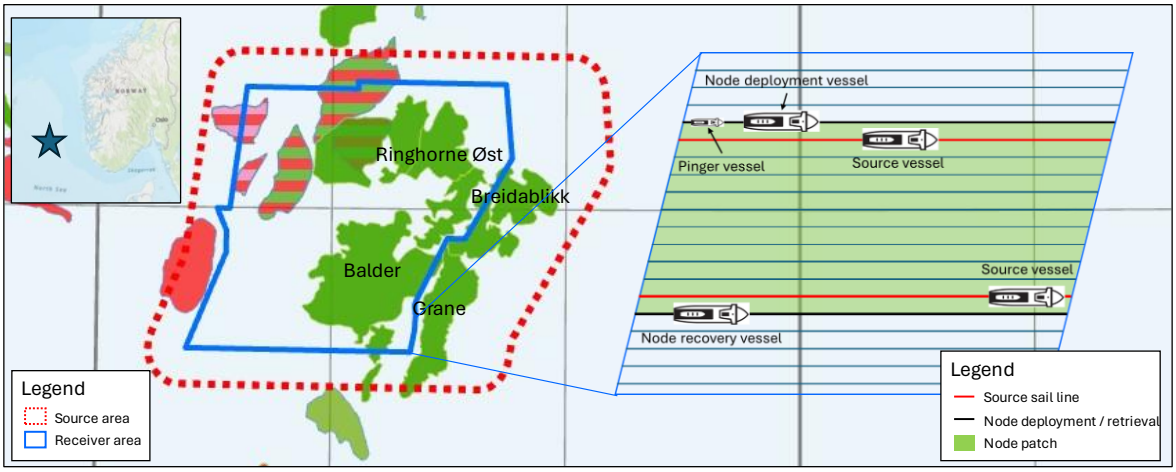

Figure 1 *Map showing node and source areas. Vessel operations in the illustration to the right. Node spacing was fixed at 50 meters inline in the E-W direction and 300 meters crossline, whereas minimum source offset into the receivers was set at 3 km in the north, west and south, and 8 km in the east.*

The survey was acquired with a total of nine vessels: three node handling vessels (NHV), two source vessels (SV), two remotely operated vehicle (ROV) vessels, one guard vessel and one supply vessel. Three different receiver types were used to record data and used as input to data processing. Whereas the bulk of the nodes were deployed using nodes on a rope (NOAR), 286 nodes were deployed by ROV in proximity to surface and subsea obstructions where NOAR was not feasible. The final input to processing was recorded in parts of the permanent reservoir monitoring (PRM) system installed on the Grane field to the east, where node deployment was not permitted.

The aim of this paper is to show that 1) OBN surveys can be successfully executed in parallel with other simultaneous operations so long as all relevant parties are involved in the survey planning and there is sufficient communication prior to and during the operations and 2) data from several different node and receiver types with input from multiple source vessels can be successfully processed to meet the objectives of the survey.

Motivation

The Balder field, operated by Vår Energi, is located in the first awarded license in the Norwegian North Sea and has produced oil since 1999. The main reservoirs (as well as for the neighbouring Ringhorne field also operated by Vår Energi) consist of large Paleocene mounds of sand as well as interconnected, remobilized and injected Eocene sands. Current development projects aim at extending the production in the area to 2045. The portfolio of drilling opportunities in the Balder area includes targets in relatively thin, steeply dipping, injectite bodies. Existing proprietary towed streamer surveys (a conventional 3D survey acquired in 2001 as well as four subsequent monitor surveys) have geometry shortcomings that make imaging of such steep injectites challenging. These narrow-azimuth, short- offset (2.5 km) surveys

limit the applicability of modern imaging techniques such as Full Waveform Inversion (FWI). Existing multi-azimuth streamer surveys, including proprietary dual-azimuth co-processing of the 2001 survey with an orthogonal survey have shown promising imaging uplifts but exhibit large coverage gaps caused by the presence of Balder Floating Production Unit (FPU), Ringhorne and nearby Grane platforms. In addition, with on-going development and exploration drilling campaigns, one to two semi-submersible drilling rigs would further impair any new long-offset, wide-spread, single or multi-azimuth streamer survey. With such operational constraints, and a need for long-offset, multi-azimuth data, it was decided to acquire a large OBN survey, covering the Balder and Ringhorne fields as well as other nearby prospective areas.

Acquisition

During the planning phase, it became apparent that there were multiple other operations planned within and adjacent to the survey area. To avoid simultaneous operations, the survey was carefully designed not to interfere with these, including 1) drilling, which included moving of the drilling rig between two sites within the survey area, 2) diving activities and 3) scheduled source acquisition over the receivers on the Grane PRM survey immediately to the east.

Simultaneous shooting was implemented to maximise the acquisition time available whilst improving the quality of the image with denser shot spacing, resulting in better signal-to-noise ratio. Two source vessels, each equipped with three airgun arrays towed with 50 meters separation, fired at 25 meters shot point intervals (8.33m flip-to-flop-to-flap shot point interval). The two SV were separated by a minimum of 2700 m in both crossline and inline directions, with a 0.2 knot speed differential and a dithering of +/- 400 ms. This set-up allowed the simultaneous shooting to be randomised in the receiver gather domain, to ease deblending.

Prior to survey start, 286 nodes were deployed by ROV in proximity to anchors and other seabed or suspended obstructions to facilitate undershooting of the Balder FPU and a drilling rig. The main survey started on April 20, when the first of 74 receiver lines was deployed using NOAR to cover the remaining area outside where nodes had already been deployed by ROV. Starting in the south with two NHV, nodes were deployed in receiver lines laid out in patches of minimum 10 to maintain a crossline offset of minimum 3 kilometers. Two SV operated in H-pattern around the node carpet while the node patches were moved sequentially from south to north through the survey area, deviating around surface and subsurface obstructions where necessary. When the final node was recovered on June 14, a total of 28,814 node positions had been recorded and a total of 1,175,972 sources had been fired. More than 96% of the nodes were successfully deployed within the positioning tolerance defined as 10% of water depth plus 5 meters relative to pre-plot.

Despite careful planning, the recorded data was significantly more affected by the source effort on the Grane PRM than planned. Advanced processing steps, including source deblending and noise removal, were applied to the three node types to mitigate the acquisition challenges and achieve the objectives of the survey.

Initial Processing Results

All 28,814 nodes were processed through a fast-track processing sequence, including deblending, Up-Down Deconvolution (UDD), and imaging of the UDD data using 40 Hz RTM. The velocity model used for the fast-track migration was generated using least-squares diving-wave FWI up to 9 Hz above the maximum depth of penetration of diving waves. This was followed by Time-lag FWI (TLFWI; Zhang et al., 2018) up to 10 Hz, utilizing the full recorded wavefield, including diving waves, ghosts, multiples and primary energy, to invert for high-frequency details at all depths.

Deblending was applied in the common-receiver domain and involved modelling the cross-talk noise using an inversion scheme, followed by an impulsive denoising phase. Figure 2 shows a 3D stack of hydrophone data before and after deblending. The deblending algorithm effectively attenuated cross-talk noise from the following shot (N+1) that saturated the deeper section, as well as the noise from the second shooting vessel that contaminated the whole section.

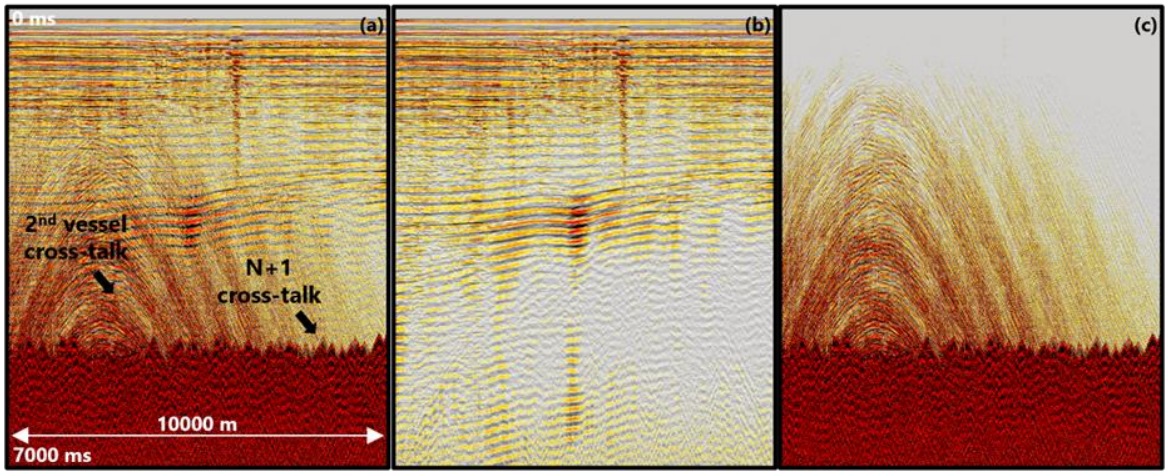

Figure 2 *3D stack of the hydrophone component (a) before and (b) after deblending, and (c) difference, showing effective attenuation of cross-talk noise.*

After deblending, the hydrophone and vertical geophone recordings were processed through geophone rotation, receiver and shot repositioning, and shot regularisation to a 12.5 × 12.5 m grid with spatial anti-aliasing. The two components were then calibrated. A typical calibration process requires application of a sensitivity correction scalar, a global geophone-to-hydrophone scalar and filter, and an instrument response inverse filter to synchronize the two components and remove the non-linear phase response of the recordings. Due to differences in specification between the NOAR and ROV nodes, the two types of nodes required different scalars and filters for calibration. In addition, a global scalar was applied to the ROV nodes to match to the NOAR nodes, to synchronize the hydrophone and vertical geophone components of the two types of nodes prior to UDD (Figure 3a). To complete the required output area, data from four receiver lines belonging to the Grane PRM system in the east, where node deployment was restricted, were also incorporated and matched to the main data to produce a continuous seamless volume (Figure 3b).

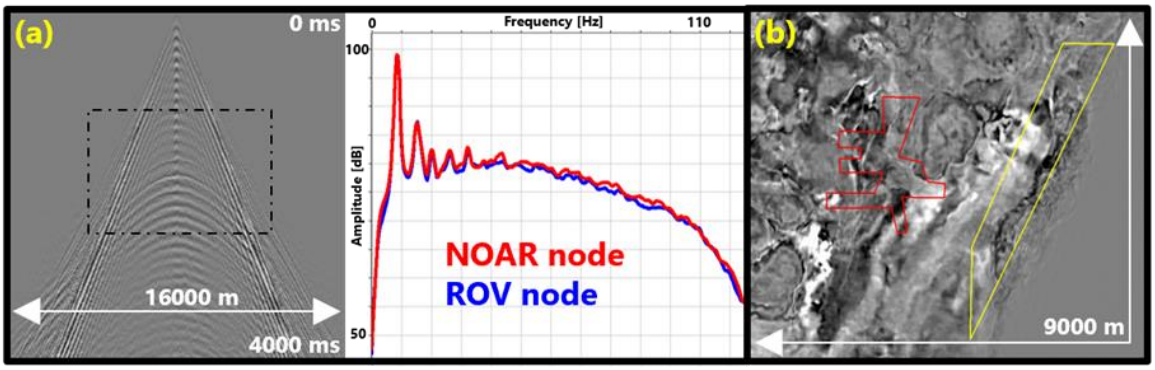

Figure 3 *(a) Amplitude spectra computed from the hydrophone component of a receiver gather after calibration and matching of ROV to NOAR nodes; (b) 1756 ms time slice from the final 40 Hz RTM stack of the Up-Down deconvolution data, highlighting in red the area covered by ROV nodes and in yellow the area belonging to the Grane PRM system.*

The hydrophone and vertical geophone components were finally summed and subtracted to calculate up-going and down-going wavefields, respectively. Both wavefields were input to UDD, to attenuate free-surface multiples and remove the source ghost and signature effects, without use of adaptive subtraction.

Up-down deconvolution data were imaged using a 40 Hz RTM using a 35-degree pre-migration angle mute. Post-migration processing included machine learning guided denoise (Hou and Messud, 2021) and amplitude Q compensation (see Figure 4a). The final stack was compared to the Kirchhoff PSDM stack of the legacy 2001 survey reprocessed in 2020 (Figure 4b). The comparison shows an

improvement in structural imaging, mainly in the Jurassic sediments below 2000 m (green arrows), and a reduction of short wavelength distortions at Top Shetland (red arrows) due to the high-frequency details captured in the imaging velocity model. Improvements in illumination due to the multi-azimuth nature of the OBN acquisition (Figure 4c) were also visible in the comparison to SAZ data (Figure 4d), with no wave-fronting artefacts observed in the node data, which would otherwise compromise the interpretation of the Paleocene sands of interest (orange arrows).

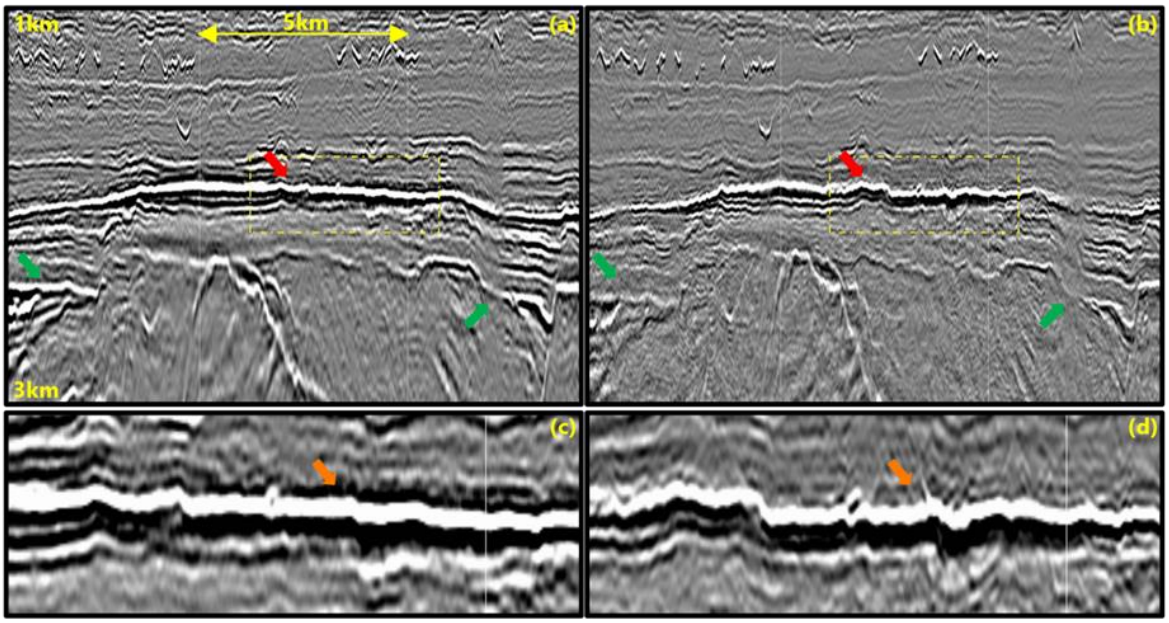

Figure 4 *(a) and (c) 40 Hz RTM stack in depth of the OBN Up-Down deconvolution data; (b) and (d) SAZ towed-streamer Kirchhoff stack in depth with 40 Hz low-pass filter applied for easier comparison. Comparison shows improvement in illumination and structural imaging.*

Conclusions

The current case shows that acquisition of OBN data in the vicinity of field infrastructure and concurrent field operations may be complex and challenging, but that the challenges may be mitigated through careful planning and coordination in dialog with multiple operations teams before and during the operations. Whereas the data acquired as part of the Heimdal Terrace OBN survey was significantly affected by the source effort on the adjacent Grane PRM, the first processing results show that advanced processing can leverage those challenges and deliver promising fast-track data.

Acknowledgements

The authors wish to acknowledge colleagues in Vår Energi, CGG and TGS for their contribution to this paper. Fast-track processing results courtesy of CGG Subsurface Imaging. Colleagues from ENI (Dario Rosa and Francesco Lo Duca) are thanked for their fruitful discussions during processing, SAE for their contribution to the data acquisition, and Vår Energi ASA and Kistos Norway AS for permission to share data examples.

References

Hou, S. and Messud, J. [2021] Machine learning for seismic processing: The path to fulfilling promises. *91st SEG Annual International Meeting*, Expanded Abstracts, 3204-3208.

Jansen, S., Ramírez, A., Went, D. and Alaei, B. [2021] Benefits of using dense OBN for exploration: an example from Utsira using AI and machine learning. *First Break*. 39. 45-52.

Zhang, Z., Mei, J., Lin, F., Huang, R. and Wang, P. [2018] Correcting for salt misinterpretation with full-waveform inversion. *88th SEG Annual International Meeting*, Expanded Abstracts, 1143-1147.